ISSN 2706-6827 Vol. 3, Issue 17: 127-134, DOI: 10.25236/IJFS.2021.031719

Energy Dissipation Analysis of FRP Concrete Steel Tube under Multiple Impact

Guoliang Zhai[1,3,a*], Ping Lu[1,2,b], Haibo Wang[3,c], Shilei Zhang[1,d], Manli Zhang[1,e]

[1]School of Architectural Engineering, Zhengzhou University of Industrial Technology, Zhengzhou 451150, Henan, China
[2]School of management Science and Engineering, Zhengzhou University, Zhengzhou 450001, Henan, China
[3]School of Civil and Architectural Engineering, Anhui University of Science & Technology, Huainan 232001, Anhui, China
[a]027069@zzgyxy.edu.cn, [b]1554971157@qq.com, [c]wanghb_aust@163.com, [d]2593290604@qq.com, [e]245093939@qq.com
**corresponding author*

Abstract: *In order to study the effects of wall thickness and impact times on the splitting tensile properties of FRP pipe concrete steel pipe, the dynamic impact test of FRP pipe concrete steel pipe is carried out by using the separated Hopkinson compression bar system with a diameter of 74mm. By changing the wall thickness and impact times, the variation laws of FRP concrete dynamic characteristics under different conditions are analyzed. The test results show that the increase of FRP pipe thickness greatly improves the load resistance of the specimen, the increase of FRP pipe thickness greatly improves the toughness and fatigue resistance of the specimen, and the energy absorption capacity of FRP pipe material is better than that of concrete; In terms of failure mode, the increase of FRP pipe thickness significantly enhances the protection ability of the specimen.*

Keyword: *FRP pipe concrete steel pipe, SHPB, Energy dissipation, Crushing form.*

Fiber reinforced polymer (FRP) is a composite material made of polymer epoxy resin, glass fiber reinforced plastic and carbon fiber. In order to improve the performance of concrete, FRP pipe is widely used in concrete structure engineering. Therefore, the research of FRP pipe concrete steel pipe is in a period of rapid development.

Rizkalla et al. [1] proposed an analytical model to predict the mechanical performance of FRP concrete-filled tubular columns under axial load. In addition to the above research on the compressive properties of FRP pipe confined concrete, many experts also study its flexural properties and composite mechanical properties. Hong et al. [2] studied the effects of FRP pipe wall thickness and filament winding angle on its stress and strain through the bending test of FRP pipe confined concrete. Che yuan [3] made an in-depth study of the specimens and obtained the types and characteristics of steel beam joints of CFRP pipe concrete filled steel tubular columns, the design principles of steel beam joints of CFRP pipe concrete filled steel tubular columns, and the research status of steel beam joints of CFRP pipe concrete filled steel tubular columns. Shi Yatao [4] found the law of the change of column bearing capacity. With the increase of the thickness of the middle part of the circular arc mortar surface of the square steel pipe, the vertical bearing capacity of the component is greatly improved. It provides a theoretical basis for strengthening or repairing the columns that play a bearing role, and further improves the theory of column bearing capacity. Mingxue Liu [5] selected three specimens to study the bending performance of FRP pipe concrete steel pipe combination. The theoretical calculation formula of flexural strength is proposed. The simplified formula of flexural strength of composite structure is obtained by test, simulation and theoretical analysis, and the three line moment curvature model is expressed as a function of flexural stiffness of composite structure section. It provides theoretical support for the shear bearing capacity of beams and columns with large slenderness ratio, which makes the application of such members into production and life an important step. T. Yu [6] et al. Proposed a new type of FRP pipe concrete steel double-layer pipe column. Compared with conventional columns and new composite columns, the ductility, bearing capacity, shear capacity and corrosion resistance of new composite columns are much higher than those of conventional columns. According to the existing test results and the results of finite element model through simulation calculation, a stress-strain model with restraint effect on concrete is proposed, which has good practical value and can be provided to

ISSN 2706-6827 Vol. 3, Issue 17: 127-134, DOI: 10.25236/IJFS.2021.031719

practical designers for design. Togay ozbakkaloglu [7] studied the compression performance of FRP pipe concrete steel double-layer pipe column structure. The parameters such as the thickness of FRP pipe, concrete strength and whether the concrete filling is dense will affect the test results. Steel pipe and FRP pipe have good restraint ability to concrete, so that concrete has better ductility and compression performance. J. Yao [8] studied the influence of load eccentricity and restraint stiffness on the specimen. Eccentric compression will greatly improve the ductility of the specimen, and the increase of eccentric load will reduce the axial bearing capacity and resistance to deformation; However, the increase of restraint stiffness will significantly improve the bearing capacity and deformation resistance. Tao Yu [9] proposed a new development concept, namely FRP pipe concrete steel multi tube concrete column (MTCC). MTCC is composed of an external FRP pipe and several internal steel pipes, and the remaining space between the steel pipes is filled with concrete. The external FRP pipe protects the internal steel pipe, which greatly improves its excellent performance. After the concrete is constrained by both, the bearing capacity and failure performance of concrete are greatly improved. The test results show that the concrete in the test column is effectively restrained and the yield of steel pipe is effectively prevented, resulting in the ductile response of the column.

Both domestic and foreign studies on energy dissipation are based on three wave method and two wave method [10-12]. It explains countless phenomena, obtains a lot of research results, and promotes the progress of theory and the development of society.

1. SHPB Test Theory

1.1. SHPB Test Device

The split Hopkinson pressure bar device shown in Figure 1 is used in this test, which is a variable section SHPB test. The pressure bar with a diameter of 74mm is selected. The transition length from the small end to the large end of the incident bar is 400mm and the large end is 2700mm; The diameter and length of the transmission rod are 1800mm. The elastic modulus is 210 GPA and the longitudinal wave velocity is 5190 m / s.

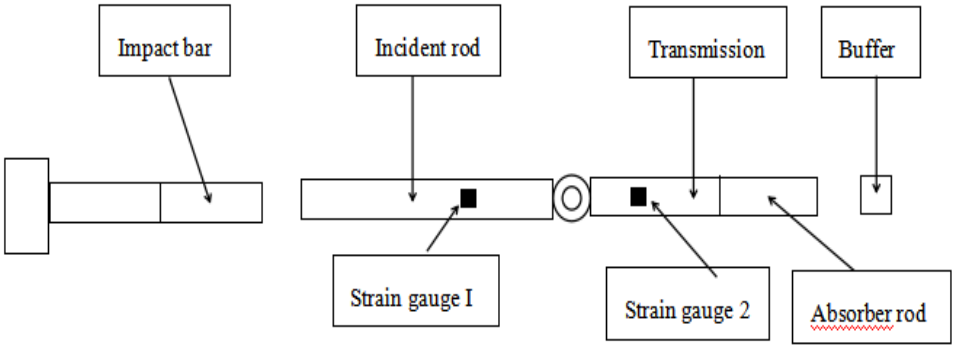

Figure 1: SHPB test device system diagram

1.2. Energy Dissipation Theory

The nitrogen is flushed into the air pressure chamber, and the nitrogen is released when it reaches a certain pressure. The nitrogen pushes the impact rod to impact the incident rod at a certain speed in a certain direction. The kinetic energy of the impact rod is the source of the energy of the rear rod. During impact, the kinetic energy of the impact rod is transformed into the internal energy of the rod for transmission.

$$W = \frac{1}{2}\mathrm{m}v_0^2 = \frac{1}{2}\pi R^2 L\rho v_0^2 \tag{1}$$

Where: W is the kinetic energy of the impact rod; m is mass of impact bar; v_o is the speed of the impact bar; R is the radius of the impact bar; L is the length of the impact bar; ρ is the density of the impact bar.

ISSN 2706-6827 Vol. 3, Issue 17: 127-134, DOI: 10.25236/IJFS.2021.031719

During the dynamic test, the energy of the incident wave is transmitted to the reflecting rod, the transmitting rod, the crushing energy, thermal energy and kinetic energy of the specimen.

$$W_I = W_R + W_T + W_S + W_F + W_K + W_M \tag{2}$$

Where: W_I is the incident wave energy (J); W_R is the reflected wave energy (J); W_T is the transmitted wave energy (J); W_S is absorb energy for the test piece (J); W_F is heat energy (J); W_K is kinetic energy (J); W_M is other energy of the test piece (vibration, sound, etc). (J);

The fragments generated during the failure of the specimen fly out and part of the energy is converted into kinetic energy. According to the experimental study of SHPB dynamics by Zhang et al. [13], the energy dissipation analysis results show that the kinetic energy of the specimen accounts for only a very small part of the absorbed energy, which can be ignored. The ratio of kinetic energy to absorbed energy is:

$$:\frac{W_{\mathrm{k}}}{W_S} = \frac{(0.69V_0 + 0.22)}{100} \tag{3}$$

Where: W_{k} is kinetic energy (J); W_{S} is absorb energy for the test piece (J); V_0 is the speed of the impact bar (m/s).

According to the experimental study on SHPB dynamics by Li Miao et al. [14], the proportion of kinetic energy in absorbed energy is small and negligible, and the thermal energy and other energy are also small and negligible. It is difficult to directly measure the energy value of absorbed energy. The absorbed energy is calculated by indirect method. After removing the negligible energy, the formula of absorbed energy can be obtained from formula (4-1):

$$W_S = W_I - W_R - W_T \tag{4}$$

Where: W_S is absorb energy for the test piece (J); W_I is the incident wave energy (J); W_R is the reflected wave energy (J); W_T is the transmitted wave energy (J).

According to the theoretical formula of energy dissipation in dynamic mechanics experiments of Zhang Rongrong and Li Tongqing [15], the incident wave energy, reflected wave energy and transmitted wave energy can be obtained by integrating and calculating the incident, reflected and transmitted strain pulses respectively.

$$W_I = \frac{AC}{E}\int \sigma_I^2 dt = AEC\int \varepsilon_I^2 \mathrm{dt} \tag{5}$$

$$W_R = \frac{AC}{E}\int \sigma_R^2 dt = AEC\int \varepsilon_R^2 \mathrm{dt} \tag{6}$$

$$W_T = \frac{AC}{E}\int \sigma_T^2 dt = AEC\int \varepsilon_T^2 \mathrm{dt} \tag{7}$$

Where: A Is the cross-sectional area of the incident rod and the transmission rod; E Is the elastic modulus of incident rod and transmission rod materials; C Is the propagation velocity of stress wave in the rod; σ_I , σ_R , σ_T . They are incident wave stress, reflected wave stress and transmitted wave stress in the specimen; ε_I , ε_R , ε_T They are incident, reflected and transmitted strain pulses in the specimen.

2. Test Results and Analysis

By substituting the data obtained from the impact test into the calculation formula, the test results of

ISSN 2706-6827 Vol. 3, Issue 17: 127-134, DOI: 10.25236/IJFS.2021.031719

multiple impacts in Table 1 can be obtained.

Table 1: Energy analysis table of multiple impact

NO	Serial number	Pressure/ MPa	Speed/ m/s	FRP Tube T/mm	Incident energy / J	Reflected energy / J	Absorbed energy / J	Reflectivity	Absorptivity
D3	1	0.8	10.431	2	269.53	239.07	27.76	0.887	0.103
	2	0.8	10.213	2	263.62	180.06	80.14	0.683	0.304
	3	0.8	10.314	2	259.94	173.64	82.92	0.668	0.319
	4	0.8	10.314	2	260.35	171.05	85.65	0.657	0.329
D6	1	0.8	10.695	3	248.08	210.98	34.34	0.851	0.138
	2	0.8	10.213	3	258.93	172.71	82.86	0.667	0.320
	3	0.8	10.096	3	0.00	0.00	0.00	0.00	0.00
	4	0.8	10.082	3	259.95	169.75	86.04	0.653	0.331
D9	1	0.8	10.731	4	251.83	204.97	43.89	0.814	0.174
	2	0.8	10.082	4	263.49	176.27	82.74	0.669	0.314
	3	0.8	10.773	4	263.47	172.84	85.89	0.656	0.326
	4	0.8	10.757	4	261.05	170.47	85.89	0.653	0.329
D12	1	0.8	10.832	5	260.66	192.31	64.77	0.738	0.248
	2	0.8	10.566	5	258.91	158.45	95.54	0.612	0.369
	3	0.8	10.142	5	259.64	155.78	98.40	0.600	0.379
	4	0.8	10.199	5	260.43	155.74	98.96	0.598	0.380

2.1. Reflected Energy of Multiple Shocks

The change process of reflected energy after four impacts on the same specimen is drawn into a curve. The reflection energy time history curve is shown in Figure 2.

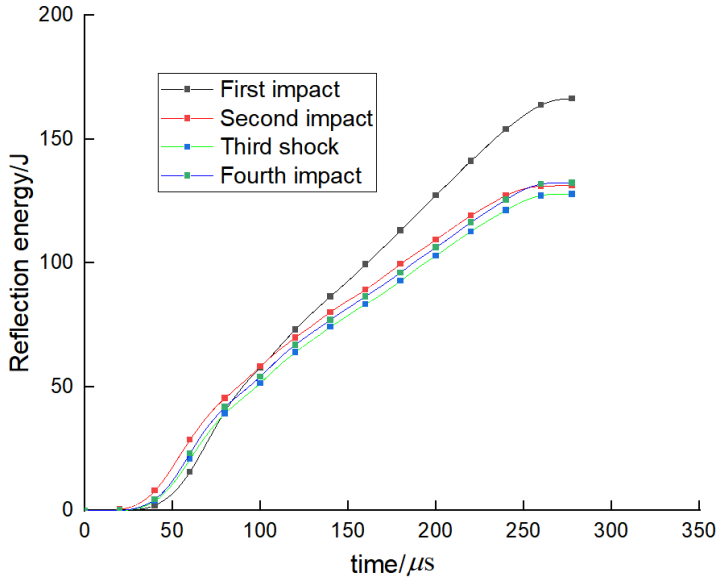

Figure 2: Time history curve of reflected energy under multiple impact

It can be seen from Figure 2 that the reflection energy is relatively high at the first impact, and the reflection energy is reduced and stable at the second, third and fourth impact. This is because the specimen deforms after the first impact, the contact area between the specimen and the compression bar increases, and the energy passing through the specimen increases, resulting in the decrease of incident energy; After the first impact, the specimen is in a stable state, and the deformation and stress distribution do not change greatly, so the reflection energy does not change much.

ISSN 2706-6827 Vol. 3, Issue 17: 127-134, DOI: 10.25236/IJFS.2021.031719

2.2. Absorbed Energy of Multiple Shocks

The change of absorbed energy of multiple impacts of the same specimen with time is drawn into an image, and the time history curve of absorbed energy is shown in Fig. 3.

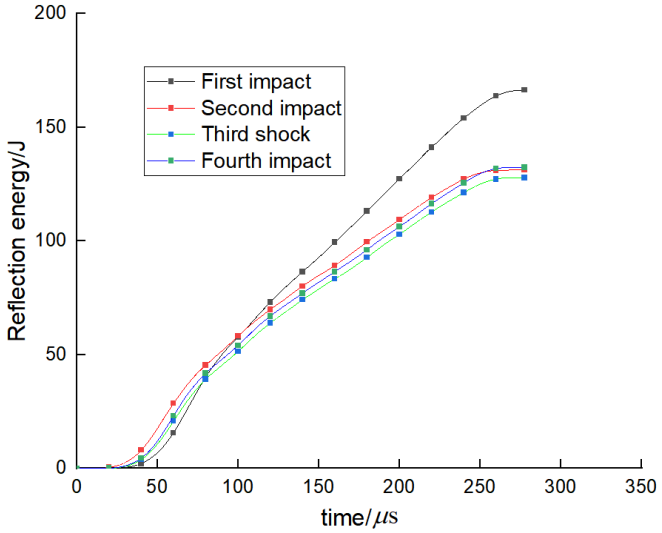

Figure 3: Time history curve of absorbed energy under multiple impact

As can be seen from Figure 3, the absorption energy is relatively low at the first impact, and increases and remains stable at the second, third and fourth impact. This is because after the first impact, the concrete in the specimen has cracks and slight crushing, which increases the absorbed energy of the specimen; The concrete is restrained by FRP pipe and steel pipe, and the specimen has strong impact resistance. Under the impact pressure of 0.8MPa, the crushing degree of concrete does not increase much, and the deformation of the specimen is not obvious, resulting in the basic consistency of the second, third and fourth absorbed energy.

2.3. Ratio of FRP Pipe Wall Thickness to Energy

Through the comparison between the first impact and multiple impacts, the relationship between the wall thickness of FRP pipe and the energy ratio is explored, as shown in Fig. 4 and Fig. 5.

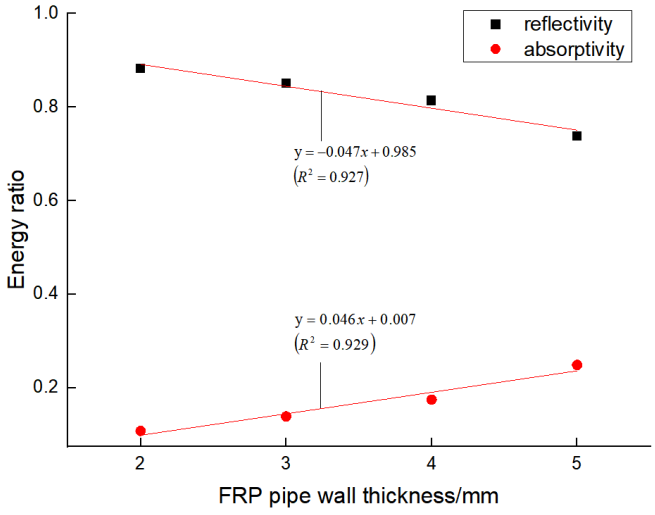

Figure 4: Relationship between FRP tube thickness and energy ratio under the first impact

ISSN 2706-6827 Vol. 3, Issue 17: 127-134, DOI: 10.25236/IJFS.2021.031719

It can be seen from Figure 4 that under the condition of the same incident energy, the reflectivity decreases linearly with the increase of FRP pipe thickness, and the absorptivity increases linearly with the increase of FRP pipe thickness. For every 1mm increase in FRP pipe wall thickness, the reflectivity decreases by 0.047 and the absorptivity increases by 0.046. This shows that the energy absorption capacity of FRP pipe material is better than that of concrete. The hardness of concrete is higher than that of FRP pipe, and the materials with low hardness have strong ability to absorb energy.

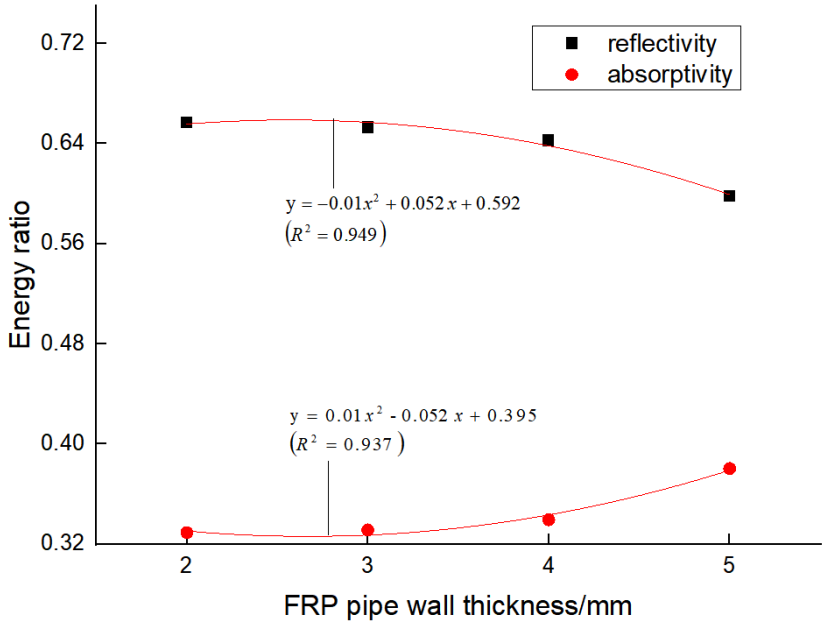

Figure 5: Relationship between FRP tube thickness and energy ratio under the first impact

It can be seen from Fig. 5 that under the condition of the same incident energy, the reflectivity decreases with the increase of the thickness of FRP tube, and the decreasing rate is faster and faster, and the absorption rate increases with the increase of the thickness of FRP tube, and the increasing rate is faster and faster.

According to the comparison between Fig. 4 and Fig. 5, after four impacts, the concrete in the specimen is damaged, the absorption capacity is enhanced, and the broken concrete is easier to absorb energy; According to the first impact, the energy absorption capacity of FRP pipe is relatively good; After repeated impact, the test block will deform, the contact area between the test block and the rod will increase, the reflected energy will decrease, and the energy absorbed by the test piece will increase. The superposition of three factors causes the increase of FRP pipe thickness to accelerate the increase of absorption energy, and the increase of FRP pipe thickness to accelerate the decrease of reflection energy.

2.4. Analysis of Crushing Morphology of Multiple Impact

Select the specimens with FRP pipe thickness of 2mm and 5mm to impact with air pressure of 0.8MPa respectively, take photos and record after each impact, and place the specimens at the same position between the two compression bars for the second, third and fourth impact. The crushing morphology of the two specimens under multiple impact is shown in Fig. 6 and Fig. 7.

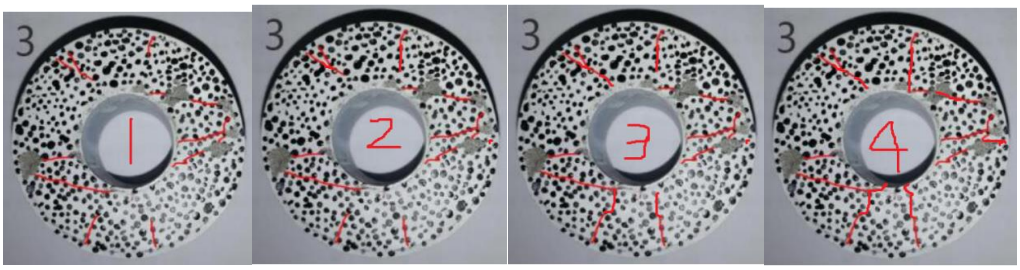

Figure 6: Fracture morphology of FRP tube under multiple impact with thickness of 2 mm

ISSN 2706-6827 Vol. 3, Issue 17: 127-134, DOI: 10.25236/IJFS.2021.031719

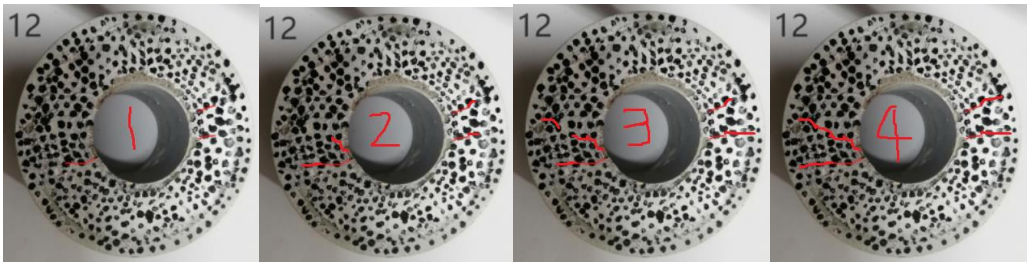

Figure 7: Fracture morphology of FRP tube under multiple impact with thickness of 5mm

As can be seen from Fig. 6, impact No. 3 test piece with 0.8MPa air pressure. For the first impact on the test piece, the concrete of the test piece was damaged and many cracks appeared, some cracks penetrated the concrete ring, a small amount of concrete fell off, and FRP pipe and steel pipe were slightly deformed; In the second impact test piece, new cracks are generated near the steel pipe, and the cracks in the upper part are developed and run through the concrete ring; For the third impact specimen, most of the cracks run through the concrete ring; For the fourth impact specimen, the cracks basically run through the concrete ring, and the deformation of FRP pipe and steel pipe increases slightly. According to the change of crushing process of No. 3 specimen under multiple impact, the concrete has been damaged during the first impact, and there is no more serious damage to the concrete under the subsequent impact, and the bearing capacity has not changed greatly. This shows that the concrete in the specimen has strong impact resistance and toughness under the protection of FRP pipe and steel pipe. The complementary advantages between the materials greatly improve the performance of the specimen. Combined with the stress-strain curve under multiple impacts, the concrete is damaged after the first impact. It is in two-way compression under the constraints of FRP pipe and steel pipe, and the specimen still has high stability.

It can be seen from Figure 7 that for the first impact test piece, there are fine cracks next to the steel pipe, the length of the cracks is also short, and the cracks do not penetrate the concrete ring; For the second, third and fourth impact test pieces, the cracks gradually develop and finally penetrate the concrete ring. There are few newly added cracks. The radial cracks of the test pieces are consistent with the axial direction of the compression bar. There are basically no cracks in the direction perpendicular to the axial direction of the compression bar. The concrete has not been broken in blocks, and the deformation of FRP pipe and steel pipe is very small. This shows that FRP pipe has good protection ability for the specimen.

It can be seen from the comparison between Fig. 6 and Fig. 7 that under the same conditions, the concrete of the specimen with FRP pipe thickness of 2mm is seriously damaged under the air pressure impact of 0.8MPa, with a large number of cracks and the falling off of block concrete. With the increase of impact times, the cracks increase more and develop faster. The concrete specimen with FRP pipe thickness of 5mm has few cracks, the increase of cracks is very small and develops slowly.

3. Conclusion

In this paper, through the uniaxial dynamic splitting tensile test of FRP pipe concrete steel pipe with different wall thickness, the following conclusions are obtained:

(1) The wall thickness of FRP pipe has a great influence on the absorbed energy and reflected energy; After the first impact, the concrete is broken and the FRP pipe and steel pipe are deformed, which increases the absorption energy and reduces the reflection energy.

(2) The increase of FRP pipe thickness greatly improves the load resistance of the specimen, and the increase of FRP pipe thickness greatly improves the toughness and fatigue resistance of the specimen.

(3) Under different FRP pipe thickness, the proportion of absorbed energy increases linearly with the increase of FRP pipe wall thickness, and the proportion of reflected energy decreases linearly; At the fourth impact, the proportion of absorbed energy increases in a quadratic parabola with the increase of FRP pipe wall thickness, and the proportion of reflected energy decreases in a quadratic parabola; Whether it is the first impact or the fourth impact, the increase of absorbed energy is roughly the same as the decrease of reflected energy.

(4) When the same specimen is impacted multiple times under the same air pressure, the reflection

ISSN 2706-6827 Vol. 3, Issue 17: 127-134, DOI: 10.25236/IJFS.2021.031719

energy is relatively high at the first impact, and decreases and remains stable at the second, third and fourth impact. The absorption energy is relatively low at the first impact, and increases and remains stable at the second, third and fourth impact.

References

[1] Sami H. Rizkalla, Amir Z. Fam. Confinement model for axially loaded concrete confined by circular fiber - reinforced polymer tubes [J]. ACI structural journal, 2001, 98(4): 451-461.
[2] Won-Kee Hong, Hee-Cheul Kim, Suk-Han Yoon. Lateral behavior of full-scale concrete-filled carbon composite columns [J]. Canadian Journal of Civil Engineering, 2004, 31(2): 189-203.
[3] Che yuan. Development of CFRP concrete filled steel tubular column steel beam joints [J]. Henan science and technology, 2020, 39(25): 90-92.
[4] Shi Yatao, Hu Zhongjun, Tan Mingrui, Li Xin, song Xuejiao. Experimental study on axial compression performance of concrete filled square steel tubular short columns restrained by CFRP sheets [J / OL]. Concrete: 1-7 [2020-12-15].
[5] Mingxue Liu, Jiaru Qian. Moment-curvature relationship of FRP-concrete-steel double-skin tubular members [J]. Frontiers of Architecture and Civil Engineering in China, 2009, 3(1).
[6] T. Yu, Y.L. Wong, J.G. Teng. Technical Papers: Behavior of Hybrid FRP-Concrete-Steel Double-Skin Tubular Columns Subjected to Eccentric Compression [J]. Advances in Structural Engineering, 2010, 13(5).
[7] Togay Ozbakkaloglu, Butje Louk Fanggi. Axial Compressive Behavior of FRP-Concrete-Steel Double-Skin Tubular Columns Made of Normal- and High-Strength Concrete [J]. Journal of Composites for Construction, 2013.
[8] J. Yao, T. Jiang, P. Xu, Z. G. Lu. Experimental Investigation on Large-scale Slender FRP-Concrete-Steel Double-Skin Tubular Columns Subjected to Eccentric Compression [J]. Advances in Structural Engineering, 2015, 18(10).
[9] Tao Yu, Chunwa Chan, Lip Teh, J. G. Teng. Hybrid FRP-Concrete-Steel Multitube Concrete Columns: Concept and Behavior [J]. Journal of Composites for Construction, 2017, 21(6).
[10] Lindholm U A. Some experiments with the split Hopkinson pressure bar [J]. Mech Phys Solid, 1964, 12(S):317-385.
[11] Song Luo, Fengqiang Gong, Li Chen. Experimental and Numerical Analyses of the Rational Loading Waveform in SHPB Test for Rock Materials [J]. Advances in Civil Engineering, 2018.
[12] Gao Hua, Xiong Chao, Yin Jun Hui. Experimental study on dynamic compressive mechanical properties of aluminum foam under repeated impact and constitutive model [J]. Journal of Ordnance Engineering, 2018, 39 (12):2410-2419.
[13] Zhang Z X, Kou S Q, Jiang L G, Effects of loading rate on rock fracture: fracture characteristics and energy partitioning [J]. International Journal of Rock Mechanics and Mining Sciences, 2000, 37(5): 745-762.
[14] Li Miao, Qiao Lan, Li Qingwen. Energy dissipation analysis of SHPB splitting test of prefabricated single joint rock under high strain rate [J]. Journal of geotechnical engineering, 2017, 39 (07): 1336-1343.
[15] Li Tongqing, Peng Yuxing. Study on crushing characteristics and energy dissipation of magnetite based on SHPB test [J]. Nonferrous metals (beneficiation), 2020 (01): 69-75.